Rocksalt or cesium chloride: Investigating the relative stability of the cesium halide structures with random phase approximation based methods

Niraj K. Nepal, Adrienn Ruzsinszky, and Jefferson E. Bates

Phys. Rev. B **97**, 115140 — Published 21 March 2018

DOI: 10.1103/PhysRevB.97.115140

Rocksalt or cesium chloride: Investigating the relative stability of the cesium halide structures with random phase approximation based methods

Niraj K. Nepal and Adrienn Ruzsinszky*

Department of Physics, Temple University,

Philadelphia, Pennsylvania 19122, United States

Jefferson E. Bates†

Department of Chemistry, Appalachian State University,

Boone, North Carolina 28607, United States

Abstract

The ground state structural and energetic properties for rocksalt and cesium chloride phases of the cesium halides were explored using the Random Phase Approximation (RPA) and beyond-RPA methods to benchmark the non-empirical SCAN meta-GGA and its empirical dispersion corrections. The importance of non-additivity and higher-order multipole moments of dispersion in these systems is discussed. RPA generally predicts the equilibrium volume for these halides within 2.4% of the experimental value, while beyond-RPA methods utilizing the renormalized adiabatic LDA (rALDA) exchange-correlation kernel are typically within 1.8%. The zero-point vibrational energy is small and shows that the stability of these halides is purely due to electronic correlation effects. The rAPBE kernel as a correction to RPA overestimates the equilibrium volume and could not predict the correct phase ordering in the case of cesium chloride, while the rALDA kernel consistently predicted results in agreement with the experiment for all of the halides. However, due to its reasonable accuracy with lower computational cost, SCAN+rVV10 proved to be a good alternative to the RPA-like methods for describing the properties of these ionic solids.

I. INTRODUCTION

Alkali halides provide a useful benchmark for new theoretical methods to test their performance in predicting equilibrium and non-equilibrium properties of ionic solids[1–7]. Among the alkali halides, cesium halides are of particular interest in terms of their phase stability and have been studied both experimentally as well as theoretically[3,8–12]. CsF is experimentally stable in the B1 structure, while the Cl, Br, and I materials exist experimentally in the B2 structure. In Strukturbericht notation, B1 corresponds to the rocksalt (NaCl) phase, whereas B2 refers to the CsCl phase[13]. This difference in phase preference for the cesium halides can only be understood through the inclusion of dispersion interactions[3,8–12].

The unexpected stability of an ionic B2 phase was explained by London[8] through the presence of relatively large van der Waals interactions between the heavy Cs^+ cation and the heavier halide anions (Cl^-, Br^-, and I^-). Since dispersion effects are proportional to the polarizability and number of electrons in the anion, they are expected to become more important as one moves down the halide column. Furthermore, the coordination number of Cs in the B2 phase is higher than that in the B1 phase so there are locally more halide anions with which to interact. Dispersion is a pure quantum mechanical effect due to instantaneous or induced electronic multipole moments and is therefore difficult to capture with classical models[14]. The simplest treatment of the dispersion interaction is modeled by simple pairwise-additive interactions between atoms, but this type of approximation completely ignores any nonadditive, nonlocal, and collective many-body effects[14,15], which can be important in cases where screening effects modify electron-electron interactions.

Rather than rely on classical models, *ab initio* calculations can be readily used to study the details of these systems. The development of accurate approximations to the exchange-correlation energy of density functional theory[16] (DFT) has enabled it to become the default electronic structure method for the computational molecular sciences. Approximations such as the local density approximation[17,18] (LDA) and the Perdew, Burke, Ernzerhof[19] (PBE) generalized gradient approximation (GGA) have been applied to a wide range of systems, but they fail to deliver accurate results when non-local interactions are important. Global hybrid density functionals, such as PBE0[20], often improve in situations with stretched bonds[21,22], but do not have any impact on dispersion interactions. By constructing meta-GGA (MGGA) approximations that include the kinetic-energy density[23–30], part of the dispersion interaction

can be directly included in a semilocal calculation, however the long-range part is still missing and must be included through other means. Incorporating the missing long-range dispersion interactions into semilocal DFT calculations by adding empirical pairwise-additive contributions has been an active topic of research for more than two decades[31–38]. More recent formulations of these corrections go beyond pairwise contributions and can include three-body terms[39] or even some non-locality[40–42].

The adiabatic-connection fluctuation-dissipation theorem (ACFDT) DFT formalism provides a non-empirical route to construct a nonlocal correlation energy that can be combined with the self-interaction free exact exchange (EXX) energy to compute the total ground state energy[43–46]. With improved algorithms[47–51] and ever increasing computational power, the Random Phase Approximation (RPA) has become an accessible alternative to semilocal DFT and is the simplest approximation within ACFDT-DFT. Naturally accounting for weak interactions, RPA has been demonstrated to yield accurate results for systems heavily influenced by van der Waals interactions (vdW)[52–56], as well as for covalently bound systems[57–63]. Since RPA is determined from a Dyson-type equation, it also naturally incorporates non-pairwise-additive dispersion contributions[64] that are missing from simple empirical dispersion schemes[45,65] and can be used as a benchmark for diverse physical and chemical properties involving both van der Waals and covalent interactions in the literature[58,66–68]. However the absence of an exchange-correlation (xc) kernel in RPA leads to an inaccurate description of short-range correlation.[69–72] Beyond-RPA (bRPA) methods including an approximate exchange-correlation kernel from time dependent DFT[45,46,72–74] (TDDFT) correct this deficiency of RPA while preserving the accurate description of long-range interactions.

In this work, we have assessed the performance of several semilocal functionals plus long-range dispersion corrections, as well as ACFDT-based methods to determine the relative stability of the cesium halides in comparison to experiment. The importance of non-additivity in these difficult ionic system was also tested. The impact of short-ranged interactions for these systems was explored with a comparative study of RPA and beyond RPA methods. The rest of the paper is organized as follows. The methods we used for this assessment are discussed in Sec. II and computational details are given in Sec. III. The results are presented in Sec. IV, followed by a brief discussion and some conclusions in Sec. V.

II. METHODS

In this work, we have used several standard semilocal functionals to assess the ground state properties of the cesium halides. Analogous to previous works[3,75], we have used the local density approximation[17] (LDA) and the generalized gradient approximation of Perdew, Burke, and Ernzerhof[19] (PBE) as a starting point for comparing the performance of more advanced methods. These two functionals do not explicitly include dispersion effects, though sometimes error cancellation in the exchange and correlation energies can simulate the effects of including these additional attractive forces[75]. Previous results reported with these functionals demonstrated that LDA predicts the correct phase ordering while PBE does not, but adding a long-range dispersion correction to PBE corrects this fundamental failure[3].

In practice dispersion corrections work well with the PBE0 global hybrid functional. PBE0 itself has been effective in

predicting the stability of hydrogen-bonded ice polymorphs[76]. Long-range dispersion corrections are, however, essential for an accurate predicition of structures for various systems. In this case PBE0 without dispersion correction does not necessarily deliver the desired accuracy as pointed out in Refs. 77–79. In order to explicitly include some dispersion at the semilocal level, more advanced approximate functionals are needed, such as from the MGGA "rung" of DFT[23,80,81].

The strongly constrained and appropriately normed (SCAN) functional is one such approximation that incorporates intermediate-range dispersion interactions through its dependence on the kinetic energy density[24]. SCAN is one of the most advanced non-empirical semilocal functionals to date, satisfying all possible exact constraints that a MGGA can, and has proven to be accurate for diversely bonded systems.[24,75,82–84] Comparing the SCAN results to those of previous non-empirical functionals should show clearly the impact that including dispersion, if only partially, makes at the semilocal level for the ground state properties of ionic materials.

Though SCAN includes intermediate-range vdW effects, it does not capture long-range interactions which arise from electron density fluctuations. To incorporate these missing contributions to the energy, we have utilized two correction schemes based on approximate treatments of the dispersion interaction. The first route, Grimme *et al.'s* D3[39,85] method, improves upon the previous D2 approach by incorporating three-body interactions and treat-

ing effects from the local environment. We also tested the impact of including dispersion through the non-local rVV10 correction[41,42,82] in combination with SCAN[24]. The rVV10 correction naturally includes higher-order multipole moments, but does not capture non-pairwise-additive effects[82]. Including the impact of these corrections is important since previous works used lower level approximations, such as D2, and found a large energy difference between the B1 and B2 phases[3].

In order to verify our semilocal results, we also utilized methods from the adiabatic-connection fluctuation-dissipation theorem (ACFDT) formulation of DFT[43,45,73,86]. The most common approximation of ACFDT-DFT, known as the Random Phase Approximation (RPA), was originally developed in the 1950's[87,88] for the uniform electron gas and has received renewed interest more recently due to increased computational power and more efficient algorithms.[47,49,50,69,89–91] The detailed mathematical description of the ACFDT formalism, as well as its implementations, can be found in the review articles Refs. 45 and 46. To summarize briefly, within the ACFDT-DFT the total energy is computed from the non-local, self-interaction-error-free exact exchange (EXX) energy and a non-local correlation energy,

$$E^{\mathrm{ACFD}} = E_{\mathrm{EXX}} + E_C^{\mathrm{ACFD}} \,. \tag{1}$$

The total correlation energy itself can be exactly decomposed into two contributions[72],

$$E_C^{\mathrm{ACFD}} = E_C^{\mathrm{RPA}} + \Delta E_C^{\mathrm{bRPA}} \,, \tag{2}$$

where the second term accounts for all of the many-body effects not captured by RPA. Within RPA, $\Delta E_C^{\mathrm{bRPA}} = 0$ since the exchange-correlation kernel is explicitly neglected. The RPA correlation energy naturally includes long-range dispersion and is non-perturbative, meaning that it can be safely applied to zero-gap systems without diverging[92]. For this work, the non-perturbative nature is important not because the band gaps are small, but because non-perturbative methods capture non-pairwise-additive contributions to dispersion[15,65]. Consequently, we can count on RPA to provide a quasi-benchmark with which to compare the semilocal and dispersion-corrected results. However, if treating the short-ranged correlation accurately is important for these ionic materials, RPA may not provide the desired accuracy needed for a true benchmark, and more advanced methods beyond RPA are needed.

Due to neglect of the exchange-correlation kernel within RPA, the short-ranged correlation is not accurately described[70,71]. To go beyond RPA, we have studied the impact of

two approximate exchange-like kernels, rALDA[93,94] and rAPBE[95]. These kernels are derived from electron gas model kernels and are spatially renormalized in order to avoid the divergence of the pair-density at the origin from adiabatic, local kernels in TDDFT.[62,73,94] These kernels have been demonstrated to improve upon RPA for non-isogyric processes, such as computing atomization or cohesive energies, while preserving the good performance of RPA for covalent and dispersion bound systems.[94–96] We have also used the CP07[97] exchange-correlation kernel to determine if the exchange-like kernels are sufficiently accurate for predicting the energy difference between the B1 and B2 phases. We did not explore the structures with these exchange-correlation kernels since they are noticably more computationally demanding and Ref. 62 demonstrated that their performance for lattice constants and bulk moduli of simple solids is only marginally different than that of rALDA and rAPBE.

Rather than compute the infinite-order response function, χ_λ, that includes the kernel[44,73,86], we utilize RPA renormalization[72,74,98] (RPAr) to compute $\Delta E_C^{\rm bRPA}$. To briefly describe these approximations, within RPA renormalization the infinite-order expression for the bRPA piece[72,74] *for a given kernel* is

$$\Delta E_C^{\rm bRPA}[f_{xc}] = -{\rm Re}\int_0^1 d\lambda \int_0^\infty \frac{du}{2\pi}\,\left\langle V\hat{\chi}_\lambda(iu) f_{xc}^\lambda(iu)\chi_\lambda(iu)\right\rangle\,, \tag{3}$$

where V is the bare Coulomb interaction, $\chi_\lambda = (1-\chi_0(V_\lambda + f_{xc}^\lambda))^{-1}\chi_0$ is the interacting density-density response function, $\hat{\chi}_\lambda = (1-\chi_0 V_\lambda)^{-1}\chi_0$ is the RPA response function, f_{xc} is the exchange-correlation kernel, iu is an imaginary frequency, though we take the Re part of the integral, λ the adiabatic-connection coupling constant, and $\langle A\rangle$ indicates the trace of matrix A. For periodic boundary conditions, this trace involves an integration over the Brillouin zone and summation over the reciprocal lattice vectors.

RPAr to first-order, RPAr1, is obtained by replacing χ_λ with the RPA response function $\hat{\chi}_\lambda$

$$\Delta E_C^{\rm RPAr1}[f_{xc}] = -\int_0^1 d\lambda \int_0^\infty \frac{du}{2\pi}\,\left\langle V\hat{\chi}_\lambda(iu) f_{xc}^\lambda(iu)\hat{\chi}_\lambda(iu)\right\rangle\,. \tag{4}$$

Note that Eq. (4) differs from Eq.(3) by the hat on the second χ_λ. RPA renormaliation to first-order (RPAr1) was previously demonstrated to account for $\sim$90 % of the total bRPA correlation energy, delivering a consistent performance in comparison to the traditional infinite-order approach[72,92,98]. In order to capture high-order correlation contributions, we have also utilized an approximate second-order RPAr correction[74] which we call the higher-

order terms (HOT) approximation.[99] This approximation makes up the difference between RPAr1 and the infinite-order result

$$\Delta E_C^{\mathrm{HOT}}[f_{xc}] = E_C^{\mathrm{bRPA}} - E_C^{\mathrm{RPAr1}} \approx -\frac{1}{2}\int_0^\infty \frac{du}{2\pi}\, \langle V\hat{\chi} f_{xc}\hat{\chi} f_{xc}\hat{\chi}\rangle \ , \tag{5}$$

typically recovering the total infinite-order correlation energy to within 1% when added to RPAr1. We have also utilized an approximation to RPAr1 called ACSOSEX[72,74,98,100–102], which neglects a certain set of third and higher-order contributions to the correlation energy in comparison to RPAr1[98]. This approximation is obtained by replacing one $\hat{\chi}$ with χ_0 in the RPAr1 correlation energy

$$\Delta E_C^{\mathrm{ACSOSEX}}[f_{xc}] = -\int_0^1 d\lambda \int_0^\infty \frac{du}{2\pi}\, \left\langle V\hat{\chi}_\lambda(iu) f_{xc}^\lambda(iu)\chi_0(iu)\right\rangle \ , \tag{6}$$

and was shown to be less systematic than RPAr1 due to the reintroduction of the non-interacting KS response function.[72,98] This is to be distinguished from the coupled-cluster doubles approximation known as second-order screened exchange[103–105] (SOSEX), however ACSOSEX and SOSEX have been shown to be analytically and numerically quite similar.[98,100] The differences in these approximations hinge on the differences in the response functions used to evaluate the traces, which can be important for describing non-perturbative dispersion interactions, since we cannot expect χ_0 to contain any information beyond the mean-field level. By studying the relative performance of these three methods we can understand the impact that the partial resummations of the correlation energy makes on the ground state properties of these ionic materials.

III. COMPUTATIONAL DETAILS

Ground state LDA and PBE calculations were performed within the Projected Augmented Wave (PAW) formalism[106] as implemented in GPAW[107–109]. We used PBE input orbitals for all of the RPA and beyond-RPA calculations, since they are evaluated non-self-consistently. Calculations with the strongly constrained and appropriately normed (SCAN) functional[24] and its combination with the revised VV10 dispersion correction (SCAN+rVV10)[82] were obtained self-consistently with VASP[110]. A plane wave cutoff of 600 eV was used in conjunction with $6 \times 6 \times 6$ Gamma-centered Monkhorst-Pack[111] k-point meshes to sample the Brillouin zone for semilocal and hybrid functionals. A higher plane

wave cutoff of 800 eV and Brillouin zone sampling of 8×8×8 were used for the EXX and RPA correlation energy calculations. Fermi-Dirac occupations corresponding to a temperature of 0.01 eV were used throughout. GPAW calculations were performed using the 0.9.20000 datasets, while the VASP calculations utilized the _sv and simple PP for Cs and halogens respectively, modified to include kinetic energy density required for MGGA calculations[112].

The non-interacting density response function can be computed from a sum-over-states expression[113] which is truncated at the number of bands determined by the plane wave cutoff for the response function. Since the calculation of the response function converges slowly with respect to the sum over unoccupied states, an extrapolation is needed to obtain converged correlation energies from the adiabatic connection.[52,69] We used a maximum cutoff for the response function of 400 eV, and 4 smaller cutoffs in 5% increments of the maximum to extrapolate the correlation energy according to Eq. (7) in Ref. 52. The frequency integral was performed as in Ref. 52 using a 16 point Gauss-Legendre quadrature, and with a frequency scale of 2.0 for non-metallic systems as recommended in Ref. 60. A Wigner-Seitz truncation scheme[114] was used for the EXX energy to treat the small wavevector divergence of the Coulomb interaction, while the perturbative approach suggested in Ref. 113 was used for the correlation energy. For the RPA correlation calculations we have used 8×8×8 Gamma-centered k-point meshes, For the bRPA calculations we have used 6×6×6 meshes for both phases because the kernel-corrected methods tend to converge faster than RPA with respect to the k-mesh size, much like the original SOSEX method[104]. We have used a 350 eV cutoff without extrapolation for these bRPA calculations. For the CP07 calculations, we used the same settings as for the rADFT kernels, but evaluated the energy difference at only a single volume for each phase near their respective minima as predicted by rALDA.

The atomic energies for the ACFD methods were computed using rectangular simulation cells of 6Å×7Å×8Å for F and 7Å×8Å×9Å for Cs, Cl, Br, and I. Two cutoffs, 300 and 350 eV, were used to extrapolate the atomic results, since these cutoffs were previously demonstrated to yield converged results for RPA.[60] Atomic EXX energies were computed using simulation cells of 12Å×12Å×12Å and an 1000 eV plane wave cutoff. The atomic energies for SCAN and SCAN+rVV10 were calculated using a plane wave basis set with maximum kinetic energies of 250–400 eV and a 20Å×20Å×20Å simulation cell.

We calculated the zero-point vibrational energy (ZPVE) from PBE using VASP and PHONOPY[115] to estimate thermal corrections to the ground state energy. The ZPVE calcu-

lation includes the effect of LO-TO splitting within a polar solid[116]. The equilibrium properties of the bulk materials were determined from a fit to the third-order Birch-Murnaghan equation of state using at least seven volume points around the minimum.

IV. RESULTS

A. Equilibrium Structural Parameters

The computed equilibrium volumes and bulk moduli are reported in Tables I and II respectively. Beyond-RPA results are computed using rALDA. Experimental volumes were obtained using the lattice constants reported in the literature[117]. PBE systematically overestimates the equilibrium volume while LDA underestimates it, and our results are in good agreement with those of Refs. 3 and 12. On the other hand, a global hybrid PBE0 does improve over PBE slightly, but still overestimates the equilibrium volume. In order to predict accurate equilibrium volumes, some level of dispersion must be included. The equilibrium volumes predicted by SCAN, SCAN+D3, and SCAN+rVV10 are much more accurate than PBE or LDA, and tend to be quite close to one another and to the RPA results. The beyond-RPA methods tend to be even more accurate than dispersion corrected SCAN or RPA in comparison to experiment. The accuracy of the various methods to estimate the bulk modulus follows essentially the same trends as for the equilibrium volumes.

B. Cohesive Energies

The cohesive energies per formula unit for the low-energy phases of the cesium halides are presented in Table III. For the fluoride this corresponds to the B1 phase, while for the other salts B2 is the low-energy phase. LDA and SCAN tend to overestimate the cohesive energies for the fluoride and chloride salts and underestimate the cohesive energy for the iodide. The bromide tends to be the halide where these semilocal functionals are closest to the experiment. PBE universally underestimates the cohesive energies for all of the halide salts. PBE0 still underestimates the cohesive energy providing only a slight improvement over PBE. Adding dispersion to PBE improves the cohesive energies of these halides[3,12]. Similarly, the D3 correction to PBE0 improves the equilibrium properties significantly, as presented in Table S5 of the supporting information[122]. Adding long range dispersion from D3 or rVV10

TABLE I. Equilibrium volumes per CsX functional unit in $Å^3$. Experimental volumes correspond to room temperature. LDA underestimates the lattice constants whereas PBE always overestimates them. RPA along with SCAN (S), S+rVV10, and S+D3 are noticably more accurate for predicting the equilibrium volumes than PBE and LDA, however the beyond-RPA methods using rALDA (RPAr1, HOT, and ACSOSEX) yield the most accurate results.

V_0	LDA	PBE	PBE0	SCAN	S+D3	S+rVV10	RPA	RPAr1	HOT	ACSOSEX	Expt.[117]
F-B1	49.299	58.096	55.844	53.783	53.443	52.849	53.566	54.118	53.959	54.027	54.270
F-B2	43.336	51.087	49.298	47.873	47.809	47.018	47.687	47.898	47.770	48.057	
Cl-B1	76.719	89.031	87.188	85.863	84.929	84.116	83.128	82.324	82.104	81.826	
Cl-B2	62.853	74.780	72.564	70.235	69.483	68.490	68.315	68.873	68.681	68.977	69.934
Br-B1	86.980	101.332	99.234	97.794	96.756	95.666	94.181	93.772	93.453	93.070	
Br-B2	71.270	84.980	82.464	79.887	78.922	77.892	77.321	78.154	78.888	78.164	78.954
I-B1	104.001	121.620	119.266	117.978	116.913	115.045	113.348	112.582	112.160	111.715	
I-B2	85.622	102.028	99.229	98.182	96.922	95.545	93.525	94.079	93.713	94.010	95.444

TABLE II. Computed bulk moduli (GPa) from the equation of state fits. The experimental values of Ref. 118 are taken at 4.2 K, Ref. 11 and 119 were measured around liquid nitrogen temperature, and the remaining were measured around room temperature. RPA and SCAN are quite accurate in predicting the bulk moduli of these halides, however SCAN+rVV10 and the kernel-corrected bRPA methods utilizing the rALDA kernel are still systematic improvements.

B	LDA	PBE	PBE0	SCAN	S+D3	S+rVV10	RPA	RPAr1	HOT	ACSOSEX	Expt.
F-B1	33.2	19.8	22.5	27.7	28.4	29.6	25.4	27.5	27.8	27.9	25.0[120]
F-B2	41.2	23.7	26.4	33.3	29.1	34.7	28.1	31.6	31.9	31.2	
Cl-B1	19.3	12.2	13.0	15.0	15.6	16.2	15.6	17.3	17.5	18.1	
Cl-B2	24.7	14.3	15.7	19.4	19.7	21.4	20.4	20.6	20.8	20.9	22.9[119]
Br-B1	16.5	10.3	11.0	12.7	13.2	13.7	13.3	14.5	14.7	15.3	
Br-B2	21.0	12.2	13.3	14.6	16.5	17.7	17.5	17.6	17.8	17.9	17.9[11], 18.4[118]
I-B1	13.3	8.2	8.7	10.0	10.4	11.0	10.8	11.8	11.9	12.4	
I-B2	16.9	9.9	10.7	13.4	12.8	13.7	13.8	14.3	14.5	14.6	13.5[121], 14.4[118]

to SCAN systematically increases the cohesive energies, resulting in larger overestimates for the fluoride and chloride, a little change for the bromide, and reducing the underestimation of the iodide salt. RPA and the bRPA methods also have varied performances, tending to yield overestimates for F and Cl, but underestimates for the Br and I salts. There is some difference amongst the bRPA methods themselves for the cohesive energies since a free atom is involved, and the different levels of RPAr recover different amounts of bRPA correlation.[74] The short-ranged contributions captured by the bRPA corrections become important for the heavier halides since the CsX bond is more covalent than the lighter halides, based solely on electronegativity differences[123]. Thus RPA tends to be more accurate vs experiment for the fluoride and chloride and less accurate for the bromide and iodide salts, whereas the bRPA methods have the opposite trend.

Comparing the semilocal results against the ACFDT results indicates that the incorporation of dispersion is crucial, as expected. The dispersion corrected SCAN results agree to a good extent with the higher level calculations, though whether they agree with RPA or bRPA methods depends on the halide. For the fluoride, the ACFDT methods are likely superior because they utilize the self-interaction error free exact exchange energy and correctly incorporate all ranges of dispersion, whereas the semilocal results (other than PBE) are too large already without dispersion and only become larger with the addition of D3 or rVV10. For the other halides, the difference between the dispersion corrected SCAN results and the bRPA methods is around 300 meV per functional unit ($\sim$3-5%) indicating an adequate prediction by the lower-level methods. Though the magnitude of the cohesive energy is important to compare with experiment, the difference in predicted cohesive energies is also important for predicting the relative stability of the B1 and B2 phases.

The differences in the predicted cohesive energies between B1 and B2 phases, $\Delta E_{\mathrm{coh}} = E_{\mathrm{coh}}^{\mathrm{B1}} - E_{\mathrm{coh}}^{\mathrm{B2}}$, are summarized in Figures 1 and 2. Figure 1 contains the dispersion-corrected semilocal results along with PBE0, and RPA. The bRPA results using rALDA are presented in Figure 2. As in Ref. 3, both PBE and PBE0 predict all of the cesium halides to prefer the B1 phase, whereas all the other methods predict CsF to prefer the B1 phase and CsCl, CsBr, and CsI to prefer the B2 phase. LDA predicts the correct energetic orderings for all of the halides in addition to accurately predicting the structural parameters. The PBE+D2 results of Ref. 3 correct the failure of PBE, but result in a large difference in cohesive energies due to an inadequate description of dispersion effects in these ionic compounds. Both

TABLE III. Computed cohesive energies (eV per formula unit) for the stable phases of the cesium halides. The columns are labeled as they were for Table I. SCAN+D3 results were computed using "zero" damping. The experimental values given by Ref. 10 are taken at room temperature.

E_{coh}	LDA	PBE	PBE0	PBE+D2[3]	SCAN	S+D3	S+rVV10	RPA	RPAr1	HOT	ACSOSEX	Expt.[10]
F B1	8.28	7.19	6.91	7.94	8.09	8.14	8.24	7.51	7.68	7.81	7.82	7.48
Cl B2	6.97	6.07	6.08	6.84	6.874	6.94	7.08	6.865	7.12	7.24	7.40	6.74
Br B2	6.49	5.64	5.70	6.48	6.37	6.44	6.57	6.03	6.08	6.20	6.42	6.48
I B2	5.92	5.12	5.20	6.02	5.73	5.80	5.94	5.56	5.59	5.70	5.93	6.18

FIG. 1. Bar diagram representing $\Delta E_{\rm coh} = E_{\rm coh}^{\rm B1} - E_{\rm coh}^{\rm B2}$ obtained with various DFT methods. PBE+D2 results are taken from Ref. 3. Positive $\Delta E_{\rm coh}$ corresponds to the B1 phase being preferred as the ground state, whereas negative values indicate the preferred stability of the B2 phase. PBE predicts all ground state cesium halides to be in the B1 phase whereas all other methods favor the B2 structure except in CsF. Data for energy differences between cohesive energies between two phases are presented by Table S1 in supplementary material[122].

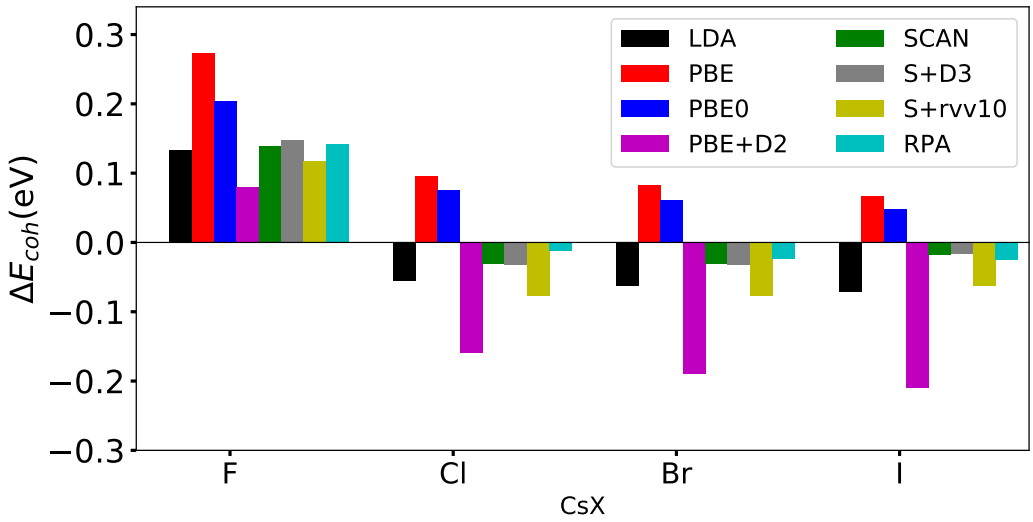

RPA and SCAN predict the correct phase ordering, but the difference in cohesive energies is noticably smaller than that of PBE+D2. RPA yields a consistent trend of increasing $\Delta E_{\rm coh}$ going down from Cl in the halide group, as do LDA and PBE+D2[3], but SCAN does not yield the same trend, with the predicted energy difference for the iodide being smaller than that for Cl and Br. Beyond RPA methods follow the RPA trend, but yield

TABLE IV. Comparison of equilibrium volumes for CsCl obtained using rAPBE with other RPA based methods.

Vol(Å^3)			rALDA			rAPBE	
	RPA	RPAr1	HOT	ACSOSEX	RPAr1	HOT	ACSOSEX
CsCl-B1	83.128	82.324	82.104	81.826	87.080	87.476	87.257
CsCl-B2	68.315	68.873	68.681	68.977	74.732	75.448	75.074

consistently larger splittings between the phases. Since the bRPA methods contain proper short- and long-ranged correlation effects, as well as a self-interaction error free exchange energy, we prefer them for a benchmark in these systems. With that in mind, the SCAN and SCAN+dispersion results yield reasonable predictions for each of the salts, though the chemical trend is not reproduced. We found that the difference in ZPVE between the two phases is 5 meV for CsF, and decreases to 0.1 meV as we go towards the heavier anions. No imaginary vibrational modes were observed during phonon calculation. These thermal shifts are negligible compared to the electronic energy difference[3], thus the primary contribution to ΔE_{coh} comes from electronic correlation at 0 K and not from any temperature effects.

The beyond RPA results obtained with the rAPBE, CDOPs, and CP07 kernels for CsCl are reported in Tables IV and V. Results for rAPBE are obtained using the Birch−Murnaghan equation of state with an energy cutoff of 350 eV, while the others were calculated close to the RPA minimum. Table IV shows that rAPBE significantly overestimates the equilibrium volume, while Table V shows that it predicts both phases to be iso-energetic, in contradiction to the experimental fact that CsCl prefers the B2 phase. Both CDOPs and CP07 predict that CsCl prefers the B2 phase by at least 15 meV per functional unit, supporting the assertion that the results obtained with the rALDA kernel are more reliable than those of rAPBE.

V. DISCUSSION & CONCLUSION

Due to the lack of explicit treatment of weak, but important, van der Waals interactions between the ions[3,9,12], PBE and PBE0 are inaccurate for determining the equilibrium ground state properties of the cesium halides. The correct ordering predicted by LDA, in addition to

TABLE V. Beyond RPA results for equilibrium energy difference ($\Delta E_{\rm coh} = E^{\rm B1}_{\rm coh} - E^{\rm B2}_{\rm coh}$) with rAPBE, CDOP, and CP07 kernels. The Birch-Murnaghan equation of state was fit to get the rAPBE results, whereas the calculation was only done near the equilibrium volume obtained with RPA for the others. Only rAPBE fails to predict the correct phase ordering. The HOT approximation is not currently implemented for CP07 or CDOPs. RPA predicts a splitting of 0.0123 eV.

ΔE_{Coh} (eV/f.u.)	rAPBE	CPO7	CDOPs
RPAr1	0.003	-0.019	-0.035
HOT	0.001	—	—
ACSOSEX	0.001	-0.019	-0.040

FIG. 2. Bar diagram representing $\Delta E_{\rm coh} = E^{\rm B1}_{\rm coh} - E^{\rm B2}_{\rm coh}$ obtained with beyond RPA methods using rALDA kernel. Dispersion corrected results to SCAN (SCAN+D3 and SCAN+rVV10) and RPA results are presented alongside for the sake of comparision between various beyond rALDA approximations. Positive $\Delta E_{\rm coh}$ indicates the B1 phase is the preferred ground state, whereas negative values indicate the preferred sability of the B2 phase. Data for energy differences between cohesive energies between two phases are presented by Table S3 in supplementary material[122].

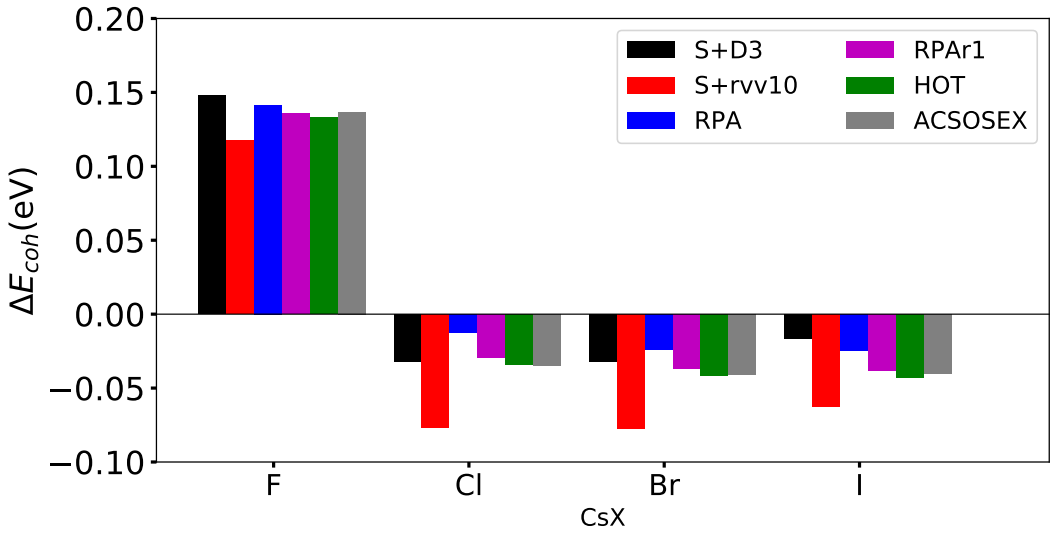

the accurate cohesive energies, is due to error cancellation between exchange and correlation, and is not reliable in general for novel ionic materials. SCAN is a reliable semilocal functional for these materials, since it incorporates some of the missing dispersion contributions absent

in the other non-empirical functionals we tested. SCAN simultaneously provides an accurate prediction of the structural properties and cohesive energies, but is unable to completely capture the same trends as RPA with respect to the relative magnitudes of the cohesive energies. Adding the long-range dispersion shifts the magnitude of the SCAN result, but does not impact its underlying physical prediction. For the cesium halides, the rVV10 correction tends to be larger in magnitude, resulting in underestimated equilibrium volumes and overestimated cohesive energies, while the D3 correction is smaller and yields overall results in close agreement with the uncorrected SCAN.

The ACFDT-DFT methods delivered highly accurate structural results, though RPA is more accurate for the cohesive properties of the lighter halogens and bRPA methods only overtake RPA for the bromide and iodide. Since RPA naturally incorporates long-range dispersion and the lighter halogens contain more ionic interactions, incorporating additional short-ranged interactions through an xc kernel overestimates the cohesive energy difference between the B1 and B2 phases. For the heavier halogens, the kernel is more important since the interactions are less ionic. Of the kernels we tested, three indicated a clear preference for the B2 phase for Cl, Br, and I, further validating our RPA and semilocal results. Though rALDA and rAPBE both share very similar functional forms, the inability of rAPBE to predict the correct phase ordering is puzzling, and will require further tests to understand. Amongst the RPAr methods there is little difference in overall performance, indicating that any reasonable treatment of bRPA effects should improve the RPA result. We prefer RPAr1 to ACSOSEX since it is a completely screened perturbation theory[72,98].

Overall, the splitting between B1 and B2 in cohesive energies predicted by LDA, RPA, SCAN, and SCAN+rVV10 ranges from 20 to 80 meV for the halogen series, whereas it ranges from 80 meV to 210 meV for PBE+D2[3] (See Fig. 1). This large splitting in PBE+D2 is due to the fact that it describes dispersion only through 2-body attractive dispersion without taking effects from local environment into account and does not incorporate repulsive 3-body dispersion contributions to the cohesive energy in these halides[124]. The lower splitting in cohesive energy by RPA and SCAN can be attributed to the fact that RPA lacks a proper description of short ranged dispersion whereas SCAN does not include long ranged dispersion. The rALDA results are more accurate for the heavier halogens than RPA because short-ranged interactions are properly included through an exchange-like kernel. The SCAN+rVV10 results also show systematic improvement over SCAN by adding missing

long-range dispersion, resulting in energy differences that closely mimic the bRPA results of rALDA. Results obtained with CP07 and CDOPs further support that the rALDA kernel is sufficiently accurate for explaining the phase stability of these ionic solids. Due to their lower computational cost, SCAN and dispersion-corrected SCAN methods can be a reliable alternative to the ACFD methods for ionic systems, where treating the various distance scales of electron-electron interactions are important. Benchmarking against RPA or bRPA is reccommended though, if one is interested in chemical trends.

ACKNOWLEDGEMENTS

We thank Chandra Shahi and Haowei Peng for their assistance with some calculations. This work was supported by the National Science Foundation under Grant No. DMR–1553022. J.E.B. was also supported through start-up funds from the A. R. Smith Chemistry Department at Appalachian State University. Computational support was provided by HPC of Temple University through the NSF major research instrumentation Grant No. CNS–09–58854. A portion of the calculations utilized resources from the Center for the Computational Design of Functional Layered Materials, an Energy Frontier Research Center (EFRC) funded by the US Department of Energy, Office of Science, Basic Energy Sciences, under Award No. DESC0012575. Figures were created using Matplotlib[125].

---

* aruzsinszky@temple.edu

† batesje@appstate.edu

[1] M. Tosi and F. Fumi, J. Phys. Chem. Solids **25**, 45 (1964).

[2] V. Luaña and L. Pueyo, Phys. Rev. B **41**, 3800 (1990).

[3] F. Zhang, J. D. Gale, B. P. Uberuaga, C. R. Stanek, and N. A. Marks, Phys. Rev. B **88**, 054112 (2013).

[4] J. Narain, N. Dwivedi, G. Agrawal, and J. Shanker, Phys. Status Solidi B **132**, 389 (1985).

[5] W. N. Mei, L. L. Boyer, M. J. Mehl, M. M. Ossowski, and H. T. Stokes, Phys. Rev. B **61**, 11425 (2000).

[6] P. Cortona, Phys. Rev. B **46**, 2008 (1992).

[7] J. M. Recio, A. M. Pendás, E. Francisco, M. Flórez, and V. Luaña, Phys. Rev. B **48**, 5891 (1993).

[8] F. London, Trans. Faraday Soc. **33**, 8b (1937).

[9] J. E. Mayer, J. Chem. Phys. **1**, 270 (1933).

[10] M. Tosi, J. Phys. Chem. Solids **24**, 965 (1963).

[11] K. Reinitz, Phys. Rev. **123**, 1615 (1961).

[12] J. Tao, F. Zheng, J. Gebhardt, J. P. Perdew, and A. M. Rappe, Phys. Rev. Materials **1**, 020802 (2017).

[13] C. Barrett and T. Massalski, *Structure of Metals 3rd revised edition: Crystallographic Methods, Principles, and Data, International Series on Materials Science and Technology, 35* (Pergamon Press, Oxford, New York, etc, 1987).

[14] J. F. Dobson, J. Comput. Chem. **114**, 1157 (2014).

[15] A. M. Reilly and A. Tkatchenko, Chem. Sci. **6**, 3289 (2015).

[16] P. Hohenberg and W. Kohn, Phys. Rev. **136**, B864 (1964).

[17] W. Kohn and L. J. Sham, Phys. Rev. **140**, A1133 (1965).

[18] U. von Barth and L. Hedin, J. Phys. C **5**, 1629 (1972).

[19] J. P. Perdew, K. Burke, and M. Ernzerhof, Phys. Rev. Lett. **77**, 3865 (1996).

[20] C. Adamo and V. Barone, J. Chem. Phys. **110**, 6158 (1999).

[21] O. A. Vydrov, G. E. Scuseria, and J. P. Perdew, J. Chem. Phys. **126**, 154109 (2007).

[22] A. J. Cohen, P. Mori-Sánchez, and W. Yang, Sci. **321**, 792 (2008).

[23] J.-D. Chai and M. Head-Gordon, Phys. Chem. Chem. Phys. **10**, 6615 (2008).

[24] J. Sun, A. Ruzsinszky, and J. P. Perdew, Phys. Rev. Lett. **115**, 036402 (2015).

[25] J. Sun, B. Xiao, and A. Ruzsinszky, J. Chem. Phys. **137**, 051101 (2012).

[26] J. Sun, B. Xiao, Y. Fang, R. Haunschild, P. Hao, A. Ruzsinszky, G. I. Csonka, G. E. Scuseria, and J. P. Perdew, Phys. Rev. Lett. **111**, 106401 (2013).

[27] Y. Zhao and D. G. Truhlar, J. Chem. Phys. **125**, 194101 (2006).

[28] Y. Zhao and D. G. Truhlar, Theor. Chem. Acc. **120**, 215 (2008).

[29] J.-D. Chai and M. Head-Gordon, Phys. Chem. Chem. Phys. **10**, 6615 (2008).

[30] J. M. del Campo, J. L. Gázquez, S. Trickey, and A. Vela, Chem. Phys. Lett. **543**, 179 (2012).

[31] Y. Andersson, D. C. Langreth, and B. I. Lundqvist, Phys. Rev. Lett. **76**, 102 (1996).

[32] Q. Wu and W. Yang, J. Chem. Phys. **116**, 515 (2002).

[33] A. D. Becke and E. R. Johnson, J. Chem. Phys. **127**, 154108 (2007).

[34] S. Grimme, J. Comput. Chem. **25**, 1463 (2004).

[35] S. Grimme, J. Comput. Chem. **27**, 1787 (2006).

[36] J. Antony and S. Grimme, Phys. Chem. Chem. Phys. **8**, 5287 (2006).

[37] A. Tkatchenko and M. Scheffler, Phys. Rev. Lett. **102**, 073005 (2009).

[38] T. Sato and H. Nakai, J. Chem. Phys. **131**, 224104 (2009).

[39] S. Grimme, J. Antony, S. Ehrlich, and H. Krieg, J. Chem. Phys. **132**, 154104 (2010).

[40] M. Dion, H. Rydberg, E. Schröder, D. C. Langreth, and B. I. Lundqvist, Phys. Rev. Lett. **92**, 246401 (2004).

[41] O. A. Vydrov and T. Van Voorhis, Phys. Rev. Lett. **103**, 063004 (2009).

[42] R. Sabatini, T. Gorni, and S. de Gironcoli, Phys. Rev. B **87**, 041108 (2013).

[43] D. C. Langreth and J. P. Perdew, Solid State Commun. **17**, 1425 (1975).

[44] D. C. Langreth and J. P. Perdew, Phys. Rev. B **15**, 2884 (1977).

[45] H. Eshuis, J. E. Bates, and F. Furche, Theor. Chem. Acc. **131**, 1084 (2012).

[46] X. Ren, P. Rinke, C. Joas, and M. Scheffler, J. Mater. Sci. **47**, 7447 (2012).

[47] H. Eshuis, J. Yarkony, and F. Furche, J. Chem. Phys. **132**, 234114 (2010).

[48] M. Del Ben, J. Hutter, and J. VandeVondele, J. Chem. Theory Comput. **9**, 2654 (2013).

[49] M. Kaltak, J. Klimeš, and G. Kresse, Phys. Rev. B **90**, 054115 (2014).

[50] M. Kállay, J. Chem. Phys. **142**, 204105 (2015).

[51] J. Wilhelm, P. Seewald, M. Del Ben, and J. Hutter, J. Chem. Theory Comput. **12**, 5851 (2016).

[52] J. Harl and G. Kresse, Phys. Rev. B **77**, 045136 (2008).

[53] L. Schimka, J. Harl, A. Stroppa, A. Grüneis, M. Marsman, F. Mittendorfer, and G. Kresse, Nat. Mater. **9**, 741 (2010).

[54] S. Lebègue, J. Harl, T. Gould, J. G. Ángyán, G. Kresse, and J. F. Dobson, Phys. Rev. Lett. **105**, 196401 (2010).

[55] H. Eshuis and F. Furche, J. Phys. Chem. Lett. **2**, 983 (2011).

[56] T. Björkman, A. Gulans, A. V. Krasheninnikov, and R. M. Nieminen, Phys. Rev. Lett. **108**, 235502 (2012).

[57] J. Harl, L. Schimka, and G. Kresse, Phys. Rev. B **81**, 115126 (2010).

[58] H. Peng and S. Lany, Phys. Rev. B **87**, 174113 (2013).

[59] L. Schimka, R. Gaudoin, J. Klimeš, M. Marsman, and G. Kresse, Phys. Rev. B **87**, 214102 (2013).

[60] T. Olsen and K. S. Thygesen, Phys. Rev. B **87**, 075111 (2013).

[61] A. M. Burow, J. E. Bates, F. Furche, and H. Eshuis, J. Chem. Theory Comput. **10**, 180 (2014).

[62] C. E. Patrick and K. S. Thygesen, J. Chem. Phys. **143**, 102802 (2015).

[63] C. E. Patrick and K. S. Thygesen, Phys. Rev. B **93**, 035133 (2016).

[64] B. M. Axilrod and E. Teller, J. Chem. Phys. **11**, 299 (1943).

[65] D. Lu, H. Nguyen, and G. Galli, J. Chem. Phys. **133**, 154110 (2010).

[66] M. Bokdam, J. Lahnsteiner, B. Ramberger, T. Schäfer, and G. Kresse, Phys. Rev. Lett. **119**, 145501 (2017).

[67] M. Casadei, X. Ren, P. Rinke, A. Rubio, and M. Scheffler, Phys. Rev. Lett. **109**, 146402 (2012).

[68] T. Björkman, A. Gulans, A. V. Krasheninnikov, and R. M. Nieminen, Phys. Rev. Lett. **108**, 235502 (2012).

[69] F. Furche, Phys. Rev. B **64**, 195120 (2001).

[70] Z. Yan, J. P. Perdew, and S. Kurth, Phys. Rev. B **61**, 16430 (2000).

[71] A. Ruzsinszky, J. P. Perdew, and G. I. Csonka, J. Chem. Theory Comput. **6**, 127 (2010).

[72] J. E. Bates, S. Laricchia, and A. Ruzsinszky, Phys. Rev. B **93**, 045119 (2016).

[73] F. Furche and T. Van Voorhis, J. Chem. Phys. **122**, 164106 (2005).

[74] J. E. Bates, J. Sensenig, and A. Ruzsinszky, Phys. Rev. B **95**, 195158 (2017).

[75] A. Patra, J. E. Bates, J. Sun, and J. P. Perdew, Proc. Nat. Acad. Sci. **114**, E9188 (2017).

[76] B. Santra, J. Klimeš, D. Alfè, A. Tkatchenko, B. Slater, A. Michaelides, R. Car, and M. Scheffler, Phys. Rev. Lett. **107**, 185701 (2011).

[77] A. Ambrosetti, A. M. Reilly, R. A. DiStasio Jr, and A. Tkatchenko, J. Chem. Phys. **140**, 18A508 (2014).

[78] A. M. Reilly and A. Tkatchenko, J. Phys. Chem. Lett. **4**, 1028 (2013).

[79] A. M. Reilly and A. Tkatchenko, J. Chem. Phys. **139**, 024705 (2013).

[80] J. P. Perdew and K. Schmidt, in *Density Functional Theory and Its Application to Materials*, Vol. 577, edited by V. Van Doren, C. Van Alsenoy, and P. Geerlings (AIP, 2001) pp. 1–20.

[81] J. Sun, R. Haunschild, B. Xiao, I. W. Bulik, G. E. Scuseria, and J. P. Perdew, J. Chem. Phys. **138**, 044113 (2013).

[82] H. Peng, Z.-H. Yang, J. P. Perdew, and J. Sun, Phys. Rev. X **6**, 041005 (2016).

[83] J. Sun, R. C. Remsing, Y. Zhang, Z. Sun, A. Ruzsinszky, H. Peng, Z. Yang, A. Paul, U. Waghmare, X. Wu, M. L. Klein, and J. P. Perdew, Nat. Chem. **8**, 831 (2016).

[84] J. G. Brandenburg, J. E. Bates, J. Sun, and J. P. Perdew, Phys. Rev. B **94**, 115144 (2016).

[85] S. Grimme, A. Hansen, J. G. Brandenburg, and C. Bannwarth, Chem. Rev. **116**, 5105 (2016).

[86] M. Lein, E. K. U. Gross, and J. P. Perdew, Phys. Rev. B **61**, 13431 (2000).

[87] D. Bohm and D. Pines, Phys. Rev. **85**, 338 (1952).

[88] D. Bohm and D. Pines, Phys. Rev. **92**, 609 (1953).

[89] F. Furche, J. Chem. Phys. **129**, 114105 (2008).

[90] D. Neuhauser, E. Rabani, and R. Baer, J. Phys. Chem. Lett. **4**, 1172 (2013).

[91] J. E. Moussa, J. Chem. Phys. **140**, 014107 (2014).

[92] N. Colonna, M. Hellgren, and S. de Gironcoli, Phys. Rev. B **90**, 125150 (2014).

[93] T. Olsen and K. S. Thygesen, Phys. Rev. B **86**, 081103(R) (2012).

[94] T. Olsen and K. S. Thygesen, Phys. Rev. B **88**, 115131 (2013).

[95] T. Olsen and K. S. Thygesen, Phys. Rev. Lett. **112**, 203001 (2014).

[96] T. S. Jauho, T. Olsen, T. Bligaard, and K. S. Thygesen, Phys. Rev. B **92**, 115140 (2015).

[97] L. A. Constantin and J. M. Pitarke, Phys. Rev. B **75**, 245127 (2007).

[98] J. E. Bates and F. Furche, J. Chem. Phys. **139**, 171103 (2013).

[99] J. E. Bates, N. Sengupta, J. Sensenig, and A. Ruzsinszky, *under review*.

[100] G. Jansen, R.-F. Liu, and J. G. Ángyán, J. Chem. Phys. **133**, 154106 (2010).

[101] J. G. Ángyán, R.-F. Liu, J. Toulouse, and G. Jansen, J. Chem. Theory Comput. **7**, 3116 (2011).

[102] X. Ren, P. Rinke, G. E. Scuseria, and M. Scheffler, Phys. Rev. B **88**, 035120 (2013).

[103] D. L. Freeman, Phys. Rev. B **15**, 5512 (1977).

[104] A. Grüneis, M. Marsman, J. Harl, L. Schimka, and G. Kresse, J. Chem. Phys. **131**, 154115 (2009).

[105] J. Paier, B. G. Janesko, T. M. Henderson, G. E. Scuseria, A. Grüneis, and G. Kresse, J. Chem. Phys. **132**, 094103 (2010).

[106] P. E. Blöchl, Phys. Rev. B **50**, 17953 (1994).

[107] M. Walter, H. Häkkinen, L. Lehtovaara, M. Puska, J. Enkovaara, C. Rostgaard, and J. J. Mortensen, J. Chem. Phys. **128**, 244101 (2008).

[108] J. J. Mortensen, L. B. Hansen, and K. W. Jacobsen, Phys. Rev. B **71**, 035109 (2005).

[109] S. R. Bahn and K. W. Jacobsen, Comput. Sci. Eng. **4**, 56 (2002).

[110] J. Hafner, J. Comput. Chem. **29**, 2044 (2008).

[111] H. J. Monkhorst and J. D. Pack, Phys. Rev. B **13**, 5188 (1976).

[112] G. Kresse and D. Joubert, Phys. Rev. B **59**, 1758 (1999).

[113] J. Yan, J. J. Mortensen, K. W. Jacobsen, and K. S. Thygesen, Phys. Rev. B **83**, 245122 (2011).

[114] R. Sundararaman and T. A. Arias, Phys. Rev. B **87**, 165122 (2013).

[115] A. Togo and I. Tanaka, Scr. Mater. **108**, 1 (2015).

[116] S. Baroni, S. De Gironcoli, A. Dal Corso, and P. Giannozzi, Rev. Mod. Phys. **73**, 515 (2001).

[117] N. W. Ashcroft and N. D. Mermin, *Solid State Physics (Holt, Rinehart and Winston, New York, 1976)* (2005) p. 403.

[118] J. Vallin, O. Beckman, and K. Salama, J. Appl. Phys. **35**, 1222 (1964).

[119] R. Singh, H. Gupta, and M. Agrawal, Phys. Rev. B **17**, 894 (1978).

[120] G. White and J. Collins, in *Proceedings of the Royal Society of London A: Mathematical, Physical and Engineering Sciences*, Vol. 333 (The Royal Society, 1973) pp. 237–259.

[121] H. K. Mao, Y. Wu, R. J. Hemley, L. C. Chen, J. F. Shu, L. W. Finger, and D. E. Cox, Phys. Rev. Lett. **64**, 1749 (1990).

[122] See Supplemental Material at [URL will be inserted by publisher] for a compressed file containing some raw data, and a pdf with data tables referenced in the main text.

[123] L. Pauling, J. Am. Chem. Soc. **54**, 3570 (1932).

[124] O. Anatole von Lilienfeld and A. Tkatchenko, J. Chem. Phys. **132**, 234109 (2010).

[125] J. D. Hunter, Comput. Sci. Eng. **9**, 90 (2007).